Atmospheric Environment 42 (2008) 8640–8650

Contents lists available at ScienceDirect

Atmospheric Environment

journal homepage: www.elsevier.com/locate/atmosenv

Dispersion study in a street canyon with tree planting by means of wind tunnel and numerical investigations – Evaluation of CFD data with experimental data

Christof Gromke[a,*], Riccardo Buccolieri[b], Silvana Di Sabatino[b], Bodo Ruck[a]

[a] Laboratory of Building and Environmental Aerodynamics, Institute for Hydromechanics, University of Karlsruhe, Kaiserstr. 12, 76128 Karlsruhe, Germany
[b] Dipartimento di Scienza dei Materiali, University of Salento, Via Monteroni, 73100 Lecce, Italy

A R T I C L E I N F O

Article history:
Received 1 February 2008
Received in revised form 28 July 2008
Accepted 13 August 2008

Keywords:
Street canyon
Tree planting
Pollutant dispersion
Wind tunnel measurements
CFD simulations
Turbulent Schmidt number

A B S T R A C T

This paper is devoted to the study of flow and traffic exhaust dispersion in urban street canyons with avenue-like tree planting. The influence of tree planting with different crown porosity was investigated. Wind tunnel experiments for perpendicular approaching flow showed that avenue-like tree planting cause increases in exhaust concentrations at the leeward wall as tree crowns reduce the vortex found in the outer regions of the tree-free street canyon and the vertically entering volume flow rate at the canyon–roof top interface. This results in less ventilation and consequently larger concentrations in proximity of the leeward wall. At the windward wall, decreases in concentration are due to the upward moving stream in front of the leeward wall which extends farther into the skimming above roof flow and is better mixed. The clean air entrained in front of the windward wall mixes with air inside the street canyon leading to smaller concentrations. Experiments performed in the wind tunnel with different tree crown porosities did not indicate substantial changes in the flow and concentration fields. The porous model crowns investigated behaved almost like impermeable objects when arranged in a sheltered position and wind speeds are relatively small as in the street canyon.

The above described experiments have been also investigated by means of numerical simulations with the CFD code FLUENT™, rarely applied to this type of problems. The standard k–ε turbulence model and the Reynolds Stress Model were used for flow while the Eulerian advection diffusion scheme has been used for dispersion. Both models reproduced qualitatively the main aspects found in wind tunnel experiments, even though they underestimated flow velocities. Improvement of CFD dispersion performance was obtained by increasing the diffusivity through the turbulent Schmidt number Sc_t. Overall we found that the k–ε model failed to capture the complex structure of dispersion process in the presence of tree planting as it would require unphysical low Sc_t values. On the other hand the RSM turbulence model agreed fairly well with experiments by slightly reducing the standard Sc_t.

The results obtained in this work by combining wind tunnel experiments and CFD based simulations to investigate this novel aspect of research suggest ways to obtain quantitative information for assessment, planning and implementation of exposure mitigation using trees in urban street canyons.

* Corresponding author. Tel.: +49 721 608 7307; fax: +49 721 608 3191.
E-mail address: gromke@ifh.uka.de (C. Gromke).

1352-2310/$ – see front matter © 2008 Elsevier Ltd. All rights reserved.
doi:10.1016/j.atmosenv.2008.08.019

1. Introduction

Traffic emissions commonly constitute the major source for air pollution in cities. Not only gaseous emissions, but also particulate matter resulting from combustion processes, abrasion of brake discs and tires as well as road dust resuspension contribute to a deterioration of air quality. This traffic-originated air pollution has a large impact on the health of the city population. Thus, strategies for ensuring air quality standards have to be developed.

In dense built-up areas, air exchange between street level and the atmospheric wind above roof top level is limited. Near ground traffic-released emissions are not effectively diluted and removed, but remain at street level, resulting in high pollutant concentrations. In this context, the question arises to what extend tree plantings in urban street canyons influence pollutant dispersion and exchange processes. Tree planting occupy considerable fractions of street canyons and, thus, may have significant effects on the natural ventilation and traffic exhaust dispersion. Dense avenue-like tree plantings with large crowns separate the lower street level from the upper roof level.

So far, a great deal of air quality studies in urban areas has been performed (Baik and Kim, 1999; Chang and Meroney, 2003; Di Sabatino et al., 2008; Eliasson et al., 2006; Gerdes and Olivari, 1999; Hanna et al., 2002; Kastner-Klein and Plate, 1999; Kastner-Klein et al., 2001; Pavageau and Schatzmann, 1999; So et al., 2005). These investigations range from large to small scale and comprise both experimental and numerical works. All studies mentioned above deal with prevailing atmospheric wind directed perpendicular to the street length axis, since this wind regime is seen to be the most critical for pollutant accumulation in street canyons. Further comprehensive overviews on this topic are given in reviews of Ahmad et al. (2005), Li et al. (2006) and Vardoulakis et al. (2003). However, the impact of vegetation, in particular that of trees in street canyons on pollutant dispersion processes has not been considered in the referred studies.

Urban street canyons with tree plantings have been addressed only in a very few studies. Numerical studies were performed by Gross (1997) and Ries and Eichhorn (2001). They both found an influence of tree planting resulting in lower flow velocities and larger pollutant concentrations. Gromke and Ruck (2007, 2008) investigated experimentally the impact of tree planting in wind tunnel studies. Measurements were performed by including as well as excluding traffic-induced turbulence which can be significant (Di Sabatino et al., 2003). When wind was approaching perpendicular to the canyon street axis, increases in pollutant concentrations at the leeward canyon wall and decreases in concentrations at the windward wall in comparison to the tree-free configuration were found. Air exchange and entrainment conditions were considerably modified, resulting in lower flow velocities and in overall larger pollutant charges inside the canyon.

In the present study, the influence of trees on the natural ventilation and pollutant dispersion within an isolated street canyon is analyzed by means of wind tunnel and numerical investigations. Experimental data were obtained from boundary layer wind tunnel experiments at an isolated street canyon model of scale 1:150 exposed to perpendicular approaching flow. A tracer gas emitting line source was embedded at street level for simulating the release of traffic exhausts. Model trees with either impermeable or permeable crowns were arranged along the canyon centre axis. Three different configurations were considered: street canyon with no vegetation, street canyon with non-porous model crowns and with porous crowns.

Numerical simulations have been performed by using the commercial CFD code FLUENT™ V6.2 (FLUENT, 2005). We consider the CFD approach to be of increasing interest and value for air quality studies on the local neighbourhood and town scale and we expect it to replace nowadays employed empirically based (prognostic) models (e.g. ADMS-family) in the near future with increasing computer power. Because of this, we employed widely used RANS models (standard k–ε and RSM) which are implemented in most of the currently used commercial CFD codes. Traffic emissions were modeled using a passive, non-reactive scalar. The turbulent mass diffusivity D_t was calculated based on the turbulent momentum diffusivity D_t and the turbulent Schmidt number Sc_t. The role of Sc_t in dispersion modeling has not been studied extensively, especially within urban areas. However, different values are reported in literature based on field and wind tunnel observations under different atmospheric stability and wind conditions, while the literature on the use in CFD models is rather poor. Recently, Tominaga and Stathopoulos (2007) reported that in previous studies the values of Sc_t spread from 0.2 to 1.3 according to the various flow properties and geometries. They concluded that an underestimation of the turbulent diffusion for scalars can be compensated by a smaller value of Sc_t. However, this type of cancellation of errors cannot be generalized, so the optimum value of Sc_t should be considered from the viewpoint of the dominant effect in the turbulent mass transport.

The starting point for CFD modelling in the present study were the results published in a previous paper by Di Sabatino et al. (2007), where FLUENT flow and pollutant dispersion in empty street canyons with different aspect ratios were analysed and compared with wind tunnel data. It was found that a turbulent Schmidt number of 0.4 is the most appropriate number for the simulation of a simple traffic source in street canyons when using the k–ε model. In this paper, we have tried to follow the same procedure for investigating flow and dispersion in street canyons with tree planting by employing the k–ε model and the RSM. In particular, based on results presented by Tominaga and Stathopoulos (2007) Sc_t values ranging from 0.2 to 1.0 have been used and their effect on computed concentrations were studied.

The overall goal of the paper is that of identifying a strategy for interpreting and supporting wind tunnel measurements in street canyons with tree planting by using a commercial CFD code such as FLUENT. It is known that wind tunnel experiments provide data only for a few number of discrete measurement points and this limit can be easily compensated by numerical simulations which allow us to easily visualize flow and concentration fields and give us information also where measurements are not available.

2. Approach

In this section, both the experimental setup of the wind tunnel investigations and the numerical modeling approach are described.

2.1. Experimental setup and measurement instrumentation

The measurements were carried out at the Laboratory of Building and Environmental Aerodynamics at the University of Karlsruhe. In an atmospheric boundary layer wind tunnel concentration and flow field measurements at a model scale street canyon have been performed. By means of vertical Irwin-type vortex generators, a horizontally ground-mounted tripping device and a fetch of 6 m length covered with roughness elements, an atmospheric boundary layer flow, typical for urban environment, was generated. In the test section, a boundary layer flow with mean velocity ($u(z)$) profile exponent $\alpha = 0.30$ and turbulence intensity (I_u) profile exponent $\alpha_I = 0.36$ according to the power law approaches (Eqs. (1) and (2)) were reproduced:

$$\frac{u(z)}{u(z_{\mathrm{ref}})} = \left(\frac{z}{z_{\mathrm{ref}}}\right)^{\alpha} \tag{1}$$

$$\frac{I_u(z)}{I_u(z_{\mathrm{ref}})} = \left(\frac{z}{z_{\mathrm{ref}}}\right)^{-\alpha_I} \tag{2}$$

The test section is 2 m wide, 1 m high, 2 m long and covered by an adjustable ceiling allowing for compensation of pressure losses in the streamwise direction. In the present investigations, a flow velocity of $u(z_{\mathrm{ref}} = H) = 4.70\ \mathrm{m\,s^{-1}}$ with H building height was realized. For more comprehensive information on the simulated atmospheric boundary layer flow, including data on the integral length scale profile $L_{ux}(z)$ and spectral distributions of turbulent kinetic energy $S_{uu}(z,f)$, see Gromke and Ruck (2005).

In the test section, a 1:150 scaled model of an isolated street canyon of length $L = 180$ m and street width $W = 18$ m with two flanking buildings of height $H = 18$ m and width $B = 18$ m was mounted perpendicular to the approaching flow (Fig. 1). Integrated in the model street, a line source, designed according to the method described in Meroney et al. (1996), was used for simulating the release of traffic exhausts. In this approach, tracer gas is streaming in a line-like camber mounted below the model setup with openings facing the street side. The homogeneity of the line source is assured by small, equidistantly spaced openings with a high pressure drop, making the tracer gas release independent of local and instantaneous pressure fluctuation at street level. In order to account for the traffic exhausts released on the sidewise street intersections, the line source exceeded the street canyon by approximately 10% on each side. The line source strength was monitored and controlled by a flow meter, ensuring a constant tracer gas supply during the measurements.

Avenue-like tree plantings were placed inside the street canyon arrangement and their influence on the dispersion of ground near released traffic exhaust and the local flow field was investigated.

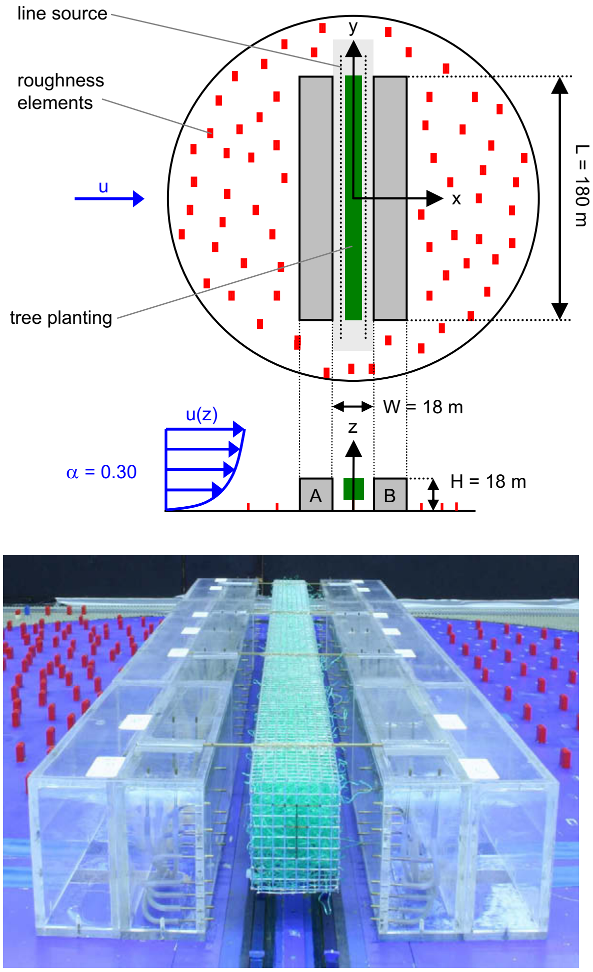

Fig. 1. Street canyon setup, scale 1:150.

Sulfur hexafluoride (SF_6) was used as tracer gas and an electron capture detector (ECD) for concentration analysis. Mean concentrations of the SF_6 gas were measured at the canyon walls and normalized according to

$$c^{+} = \frac{c u_H H}{Q/l} \tag{3}$$

with c measured concentration, H building height, u_H flow velocity at height H in the undisturbed approaching flow and Q/l tracer gas source strength per unit length. Measurements of the flow velocity inside the street canyon were performed using Laser Doppler Velocimetry (LDV). Flow velocities were normalized by the velocity of the undisturbed flow u_H at building height H.

2.2. Numerical setup and simulations

2.2.1. Computational domain, turbulence models and boundary conditions

Simulations were carried out by considering a neutral boundary layer. The computational domain was built using hexahedral elements with a finer resolution close to the ground and in those regions with large gradients (the expansion rate between two consecutive cells is below 1.3 in regions of high gradients). Several tests were performed to verify grid size independence with increasing number of mesh cells until further refinements gave no significant improvements. The final number of the computational cells used for all simulations is about 300,000. The smallest dimensions of the elements are $\delta x_{\min} = 0.05H$, $\delta y_{\min} = 0.5H$, $\delta z_{\min} = 0.05H$ in the region near the release area and near the ground. The distance from the inlet plane to the first building of the street canyon is 8H, the distance from the top of the domain to the building roof is 7H and the distance from the outflow plane to the downstream building is 30H (Fig. 2).

Two different models for simulating turbulence were used, the standard k–ε model (Launder and Spalding, 1974), which assumes isotropic turbulence, and the Reynolds Stress Model (RSM) (Launder, 1989), which calculates the individual Reynolds stresses using differential transport equations and, therefore, accounts for the differences in horizontal and vertical turbulent fluctuations.

Based on wind tunnel experiments, the inlet wind speed was assumed to follow a power law profile (Eq. (1)). Turbulent kinetic energy and dissipation rate profiles were specified as follows:

$$k = \frac{u_*^2}{\sqrt{C_\mu}}\left(1 - \frac{z}{\delta}\right) \quad (4)$$

$$\varepsilon = \frac{u_*^3}{\kappa z}\left(1 - \frac{z}{\delta}\right) \quad (5)$$

where δ is the boundary layer depth, $u_* = 0.52\ \mathrm{m\,s^{-1}}$ is the friction velocity (known from log-law curve fitting of the wind tunnel mean velocity profile), κ the von Kàrmàn

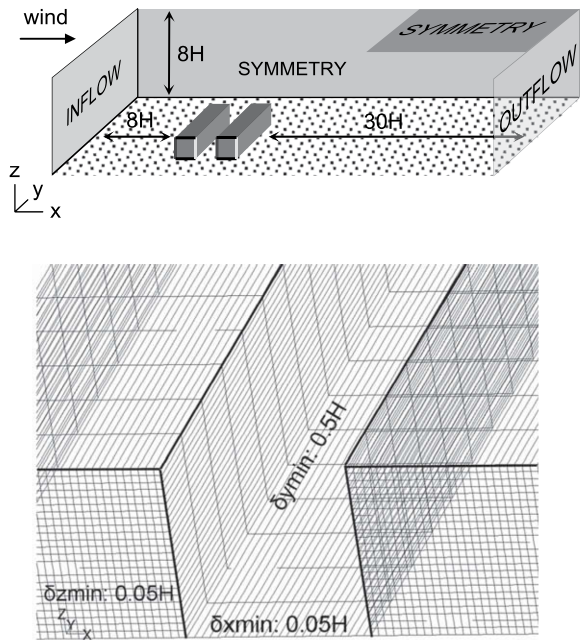

Fig. 2. Schematic sketch of geometry, boundary conditions and grid spacings used in CFD.

constant (0.4) and $C_\mu = 0.09$. When applying the RSM, FLUENT used the turbulence quantities specified in Eqs. (4) and (5) to derive the Reynolds stresses at the inlet from the assumption of isotropy of turbulence. The remaining boundary conditions were those shown in Fig. 2.

Second order upwinding discretization schemes (Barth and Jespersen, 1989) were used for pressure, momentum, k and ε to increase the accuracy and reduce numerical diffusion. The SIMPLE scheme was used for the pressure-velocity coupling. FLUENT uses an iterative method to solve the algebraic system of equations. A termination criterion of 10^{-6} was used for all field variables.

It is known that the modeling of a rough boundary layer is a challenge for typical CFD models. The simulation of a horizontal homogeneous boundary layer over rough terrain is often required in the upstream and the downstream region of the computational domain. The vertical profiles of the mean wind speed and turbulence quantities have to be maintained along the downstream distance. This occurs when the flow is in equilibrium depending on the roughness characteristics of the ground surface (Gao and Chow, 2005; Blocken et al., 2007a,b).

For the present study, accurate solutions near the ground for simulating the pollutant dispersion from a street level line source were important. In FLUENT, the surface roughness is expressed in terms of a sand grain roughness K_s instead of the roughness length z_0 as it is the case in most meteorological codes. To circumvent problems with a coarse grid resolution near the ground due to large sand grain roughness values K_s, we set K_s equal to z_0 which was found to be $z_0 = 0.0033$ m in the wind tunnel experiments. Setting K_s equal to z_0 is not correct in a strong sense; however, it is justified by the results obtained, because the inlet profiles of velocity and turbulence were maintained in a satisfactory way. With the chosen setup, we were able to maintain the inlet velocity profile free of streamwise gradients up to the location of the upstream building, with a small reduction (about 10% of the inlet values) in the region up to $z/H = 3$ for both the k–ε model and RSM. Predicted turbulence intensity tended to become smaller near the ground ($z/H < 1$), where less than 10% change were found. This can be considered acceptable in the context of our modeling approach.

Applying the k–ε turbulence closure scheme, the mean flow inside the canyon at $y/H = 0.5$ is shown in Fig. 3. A clockwise rotating vortex, driven by the above roof skimming flow, occupies the whole region within the canyon. Pollutants can be trapped within the street canyon since the exchange rate is very small.

2.2.2. Dispersion modeling

Various models are available in FLUENT to model dispersion of airborne material. In this study the advection diffusion (AD) module was used. In turbulent flows, FLUENT computes the mass diffusion as follows:

$$J = -\left(\rho D + \frac{\mu_t}{Sc_t}\right)\nabla Y \quad (6)$$

where D is the molecular diffusion coefficient for the pollutant in the mixture, $\mu_t = \rho(C_\mu k^2/\varepsilon)$ is the turbulent

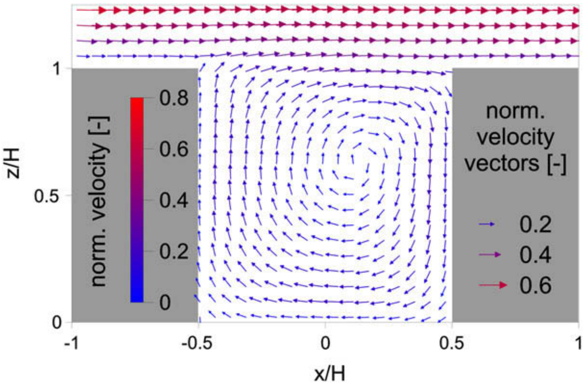

Fig. 3. Mean velocity vectors of u/u_H from FLUENT results at $y/H = 0.5$ (k–ε model).

viscosity, Y is the mass fraction of the pollutant, ρ is the mixture density. $Sc_t = \mu_t/(\rho D_t)$ is the turbulent Schmidt number, where D_t is the turbulent diffusivity. The source has been simulated by separating a volume in the geometry at the required discharge position and by setting a source term for this volume. The emission rate Q was set at $10\ \mathrm{g\,s^{-1}}$. Values for Sc_t ranging from 0.2 to 1.0 have been applied and their influence on numerically computed concentrations are studied.

3. Results and discussion

3.1. Tree-free street canyon (reference case)

3.1.1. Airflow

1-D Laser Doppler Velocimetry (LDV) has been used for velocity measurements. Inside the street canyon ($-0.5 \leq x/H \leq +0.5$, $0 \leq z/H \leq +1.3$) vertical flow field components have been acquired near the canyon center at $y/H = 0.5$. Fig. 4 shows measured and numerically calculated normalized vertical velocities $w^+ = w/u_H$.

In the contour plot of measured velocities, a downward directed flow in front of the windward side (wall B) ($0 \leq x/H \leq +0.5$) and an upward directed flow in front of the leeward side (wall A) ($-0.5 \leq x/H \leq 0$) are present. Quantitatively, the maximum vertical velocities are in the order of 25–30% of the undisturbed flow velocity at roof height u_H. As a measure for the air masses rotating with the canyon vortex, the volume flow through the horizontal plane at $z/H = 0.7$ was calculated. The volume flow per spanwise length normalized by the building height and velocity u_H amounts to roughly 0.07. The meaning of this dimensionless number is not so easy to derive. However, it is a most valuable number when comparing the flow fields in different street canyon/tree planting configurations, as will be done later.

The contour plots of the normalized vertical velocities w^+ using the k–ε and the RSM models show qualitatively similar flow fields. In comparison with the experimental results, both the turbulence models predict lower flow velocities and the air volume rotating with the canyon vortex is smaller in the numerical computations. This behavior is quantitatively the same for the two turbulence models. For example, at $z/H = 0.7$ inside the canyon, the relative deviation in normalized volume flow between measurements and numerical results is about 30%. The ventilation through the street canyon top predicted by the CFD model is too low in the idealized street canyon.

3.1.2. Pollutant concentrations

The normalized concentrations c^+ measured at the canyon walls using Electron Capture Detection (ECD) and the numerically calculated concentrations obtained with the RSM for FLUENT default turbulent Schmidt number $Sc_t = 0.7$ and $Sc_t = 0.3$ (best agreement to experimental results) are shown in Fig. 5. Similar results are obtained by using the standard k–ε model.

Large differences in pollutant concentrations can be found at the canyon walls. In the wind tunnel setup, the normalized wall-averaged traffic pollutant concentration at

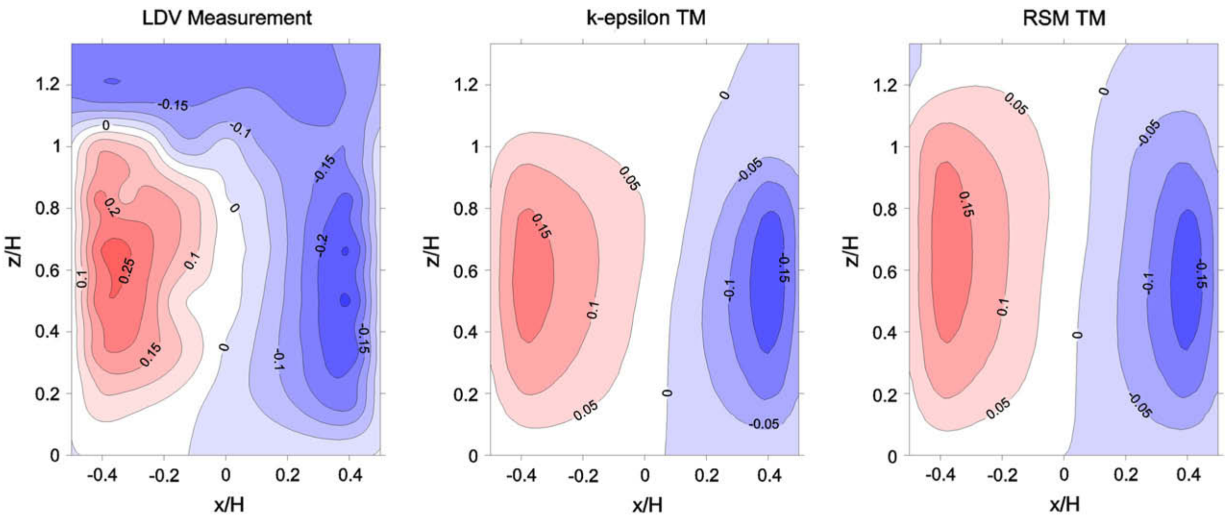

Fig. 4. Normalized vertical velocities w^+ at $y/H = 0.5$ in tree-free street canyon.

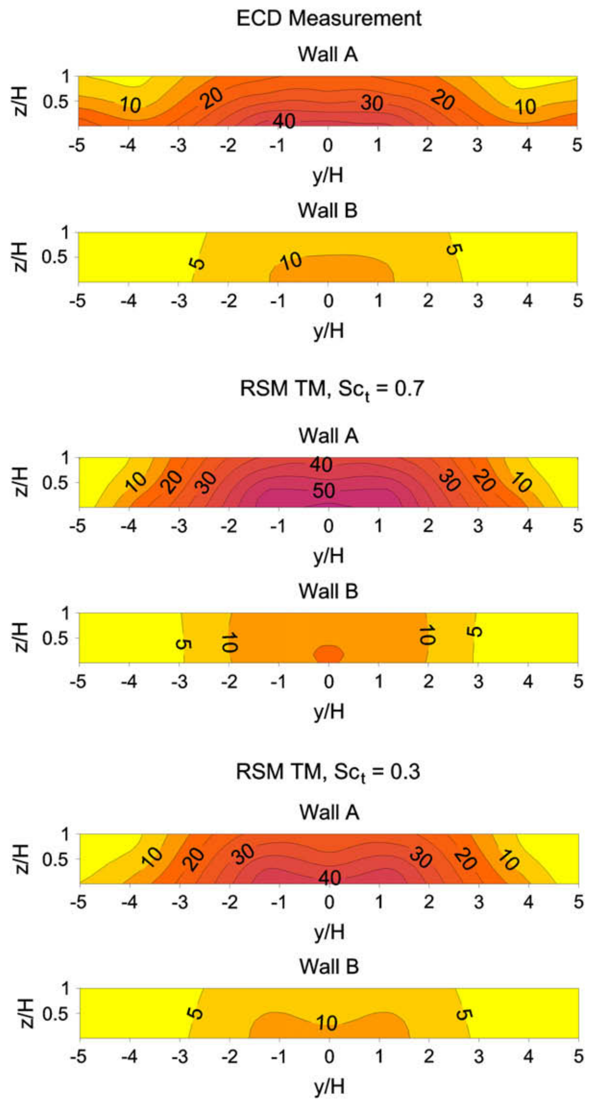

Fig. 5. Normalized concentrations c^+ at the walls of the tree-free street canyon.

wall A is $c^+_A = 19.6$ and at wall B $c^+_B = 5.4$. The near-ground released traffic exhausts get advected by the canyon vortex towards wall A. In front of wall A, the pollutants rise up and intrude in the cross flow above the roof level (Fig. 3). Here, they get mixed with the flow above and finally partially re-entrained into the street canyon in front of wall B. Thus, the pollutant charge resulting from traffic released emissions is considerably lower at wall B than at wall A. The decrease in pollutant concentrations at the canyon ends is the result of enhanced ventilation. Laterally incoming flow provides additional air exchange reducing traffic exhaust concentrations (Gromke and Ruck, 2007).

The overall FLUENT concentrations are similar to those obtained in the wind tunnel, but the actual concentration values are larger when using the standard value of Sc_t (0.7). In this case, due to the weaker canyon vortex predicted by FLUENT as shown above, less air is exchanged through the canyon top and the pollutant concentrations predicted by the numerical computation are larger. Increasing artificially the pollutant dispersion by lowering the Schmidt number from the standard value to 0.3, a closer agreement of the two models with experimental results can be achieved. In particular, the discrepancy is similar for the two turbulence models applied.

It should be noted that the change of Sc_t does not affect the turbulent momentum flux throughout the top of the street canyon, but it affects D_t in the scalar diffusion Eq. (6) and therefore it influences only the diffusion mechanism and not the fluid dynamics (as discussed in Di Sabatino et al., 2007).

3.2. Street canyon with non-porous model crown

In a next step, the street canyon with trees was investigated. An avenue-like planting of high stand density with interfering neighboring tree crowns, arranged at the street center line, was modeled. A non-porous Styrofoam block with rectangular cross section of $1/2H$ width and $2/3H$ height spanning the entire street canyon length L was tested. Between crown and building walls, a free space of $1/4H$ was remaining on each side. Below the crown bottom a distance of $1/3H$ ($\equiv 6$ m) was left to allow bigger vehicles to pass the street and the crown top was facing the building roof level. In this configuration, 1/3 of the street canyon volume is occupied by crown material.

3.2.1. Airflow

The normalized vertical velocity components w^+ near the canyon center at $y/H = 0.5$ in the presence of the non-porous, impermeable Styrofoam crown model are shown in Fig. 6. As before, in the tree-free reference case (Fig. 4), downward and upward directed flows in front of wall B and wall A, respectively, are visible. The present velocity patterns suggest the existence of canyon vortex-like structures. In the experiments, slightly smaller flow velocities in the upward but significantly lower velocities in the downward moving part are found when compared to the tree-free street canyon. The volume flow crossing the horizontal plane at $z/H = 0.7$ is reduced to a fraction of 36% of the volume flow measured in the tree-free street canyon.

In comparison with the numerical results obtained for the reference case (Fig. 4), the RSM predictions are in a better agreement with experiments than the k–ε model. For example, at $z/H = 0.7$ inside the canyon, the relative deviation in volume flow between measurements and numerical results is 16% using the RSM, while it is 50% when using the k–ε model.

3.2.2. Pollutant concentrations

The modification of the flow in the presence of trees resulted in increases in concentrations at wall A and decreases at wall B (Fig. 7). Regarding the wind tunnel results, an overall pollutant concentration rise of 48% at the canyon walls, resulting from a wall-averaged increase of 71% at the leeward wall A and a wall-averaged decrease of 35% at the windward wall B was found. The general pattern of pollutant concentration distribution remains unchanged. Maximum exhaust concentrations are present in the pedestrian level in proximity of wall A and towards the

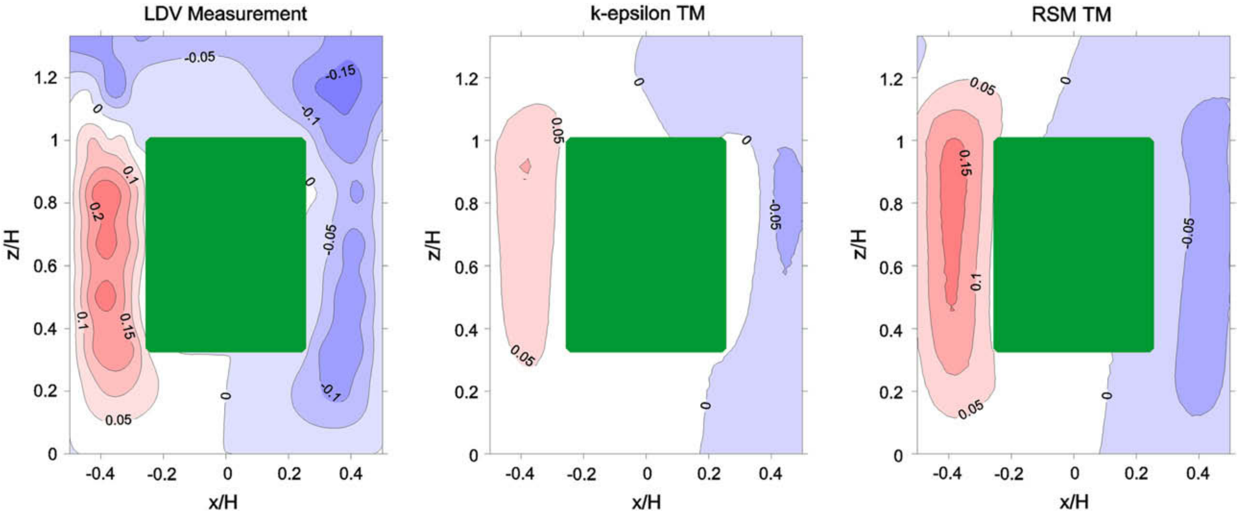

Fig. 6. Normalized vertical velocities w^{+} at $y/H=0.5$ in street canyon with non-porous tree crown model.

street canyon ends marked decreases are found. However, due to the increases in concentration at wall A and decreases at wall B, the difference in wall-average concentration between both walls is more pronounced. Whereas for the tree-free canyon the wall-average concentrations differ by a factor of 3.6, a factor of 9.6 is found for the present configuration with non-porous model crown arrangement. The difference between the tree-free and non-porous crown configuration is due to less circulating fluid mass in the case of the tree planting. Consequently, the pollutant concentration in the uprising part of the canyon vortex in front of wall A is larger. In contrary to the tree-free street canyon, no direct transport of pollutants from wall A to wall B is possible, but all of the uprising canyon vortex is intruded into the atmospheric cross flow above the roof level. Here, it is diluted before partially re-entrained into the canyon. As a consequence, lower traffic exhaust concentrations are present at wall B.

The numerical simulations with the tree planting are in qualitatively agreement with wind tunnel results, showing an increase in pollutant concentrations at wall A and a decrease at wall B, too. As before at the tree-free street canyon, a turbulent Schmidt number Sc_t parameter study was performed. Because the k–ε model performs worse, only RSM results for the default turbulent Schmidt number $Sc_t=0.7$ and $Sc_t=0.6$ (best agreement to experimental results) are shown in Fig. 7.

3.3. Street canyon with porous model crown

Real tree crowns consist of branches and leaves, which form a porous body. This porosity makes tree crowns permeable to airflow. Porous bodies show in comparison to their non-porous, i.e. solid, counterparts essentially different aerodynamic characteristics. As an example of these, porous bodies experience a larger drag and have an increased wake extension. The increase in drag is caused by the considerable larger surface of porous bodies. Their volume specific surface [$m^2\,m^{-3}$] is a multiple of that of

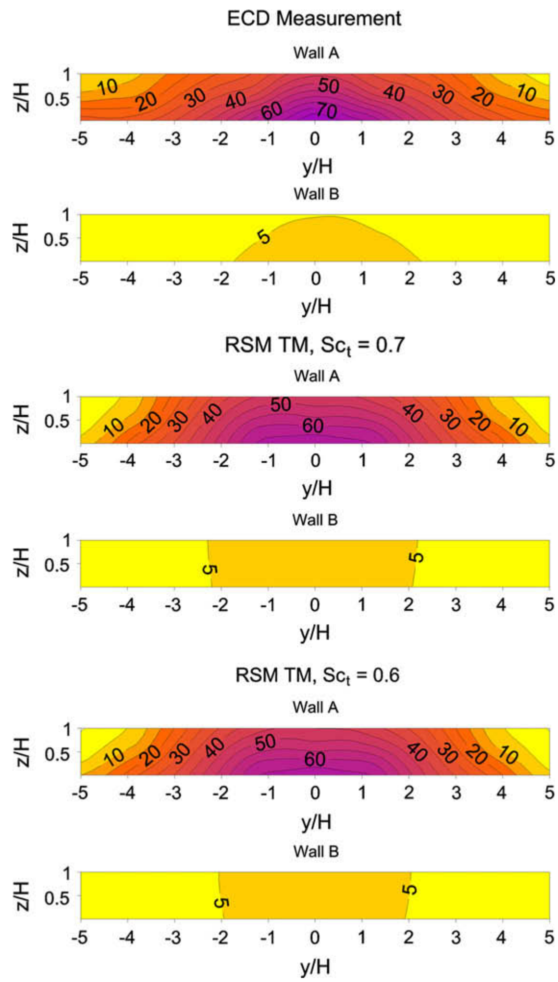

Fig. 7. Normalized concentrations c^{+} at the walls of the street canyon with non-porous crown model.

non-porous counterpart objects. Even for non-creeping flows, skin friction is important for the overall drag experienced, whereas for non-porous bodies only the difference in pressure on the windward and leeward side is relevant. Moreover, the obstacles influenced leeward flow field, the wake, extends further downstream. In comparison to non-porous bodies, the leeward flow needs a longer distance to recover from perturbations induced by porous bodies. The porosity of real tree crowns, expressed in pore volume fraction [$m^3\,m^{-3}$], roughly varies from 93% to 99%, with deciduous trees showing generally larger pore volume fractions than conifers (Gross, 1987; Ruck and Schmidt, 1986; Zhou et al., 2002).

In the present work, the porosity of tree crowns was modeled, too. For the wind tunnel investigations, an ester-based polyurethane foam 10 ppi (10 pores per inch) with a pore volume fraction of 97% was used to model porous tree crowns. A useful parameter describing the effect of porosity on permeability in terms of aerodynamic characteristics is the pressure loss coefficient λ [m^{-1}]. This coefficient is a measure of the difference in static pressure Δp_{stat} at the windward and leeward side in the case of forced convection, normalized by the dynamic pressure p_{dyn} and the body's streamwise depth d, according to

$$\lambda = \frac{\Delta p_{stat}}{p_{dyn} d} = \frac{p_{windward} - p_{leeward}}{1/2 \rho u^2 d} \tag{7}$$

with u mean velocity in streamwise direction. Measurements resulted in a pressure loss coefficient of $\lambda = 250\ m^{-1}$ for the foam ppi 10 material. For the following investigations, the non-porous model crown described in the previous chapter was replaced by a porous model crown with the above mentioned characteristics.

3.3.1. Airflow

The results of the LDV measurements and the numerical simulations in the canyon center part at $y/H = 0.5$ are shown in the contour plots of Fig. 8. As before, the velocity pattern of downward and upward directed flow in front of wall B and wall A, respectively, remains unaltered. For the wind tunnel measurements only marginal changes can be noticed in comparison to the non-porous model crown (Fig. 6). The volume flux through the horizontal plane at $z/H = 0.7$ slightly exceeds the flux measured for the non-porous model crown arrangement by 7%. Compared to the reference case (Fig. 4), the rotating fluid mass is reduced to 38%, while it is very close to the non-porous case (36%). The porous crown with pore volume fraction of 97% (or pressure loss coefficient $\lambda = 250$ Pa/(Pa m)) causes a similar flow and concentration field in the street canyon as the non-porous crown does, because the porous model crown behaves almost like an impermeable object when it is arranged in a sheltered position and wind speeds are relatively small as in the street canyon.

In FLUENT, porous media are modeled by adding a momentum source term to the standard fluid flow equations. The source term is composed of two parts: a viscous loss term and an inertial loss term. FLUENT solves the standard conservation equations for turbulence quantities in the porous medium, by treating turbulence in the medium as though the solid medium has no effect on the turbulence generation or dissipation rates. To model the considered case, we set the same block used previously as a permeable zone with the same loss coefficient as in wind tunnel experiments ($\lambda = 250\ m^{-1}$).

The contour plots of the normalized vertical velocity components w^+ inside the street canyon obtained from FLUENT using the k–ε and the RSM models are shown in Fig. 8, too. As found for the reference case and the non-porous model crown configuration before, the RSM model predictions are in closer agreement with experiments than the k–ε model. For example, inside the canyon at $z/H = 0.7$ the relative deviation in the normalized volume flow of the air circulating in the gaps between the building walls and tree crown is about +16% using the RSM model, while it is about −28% when using the k–ε model. Differently from the previous configurations investigated, the RSM closure scheme results in an overestimation of the volume flow inside the canyon.

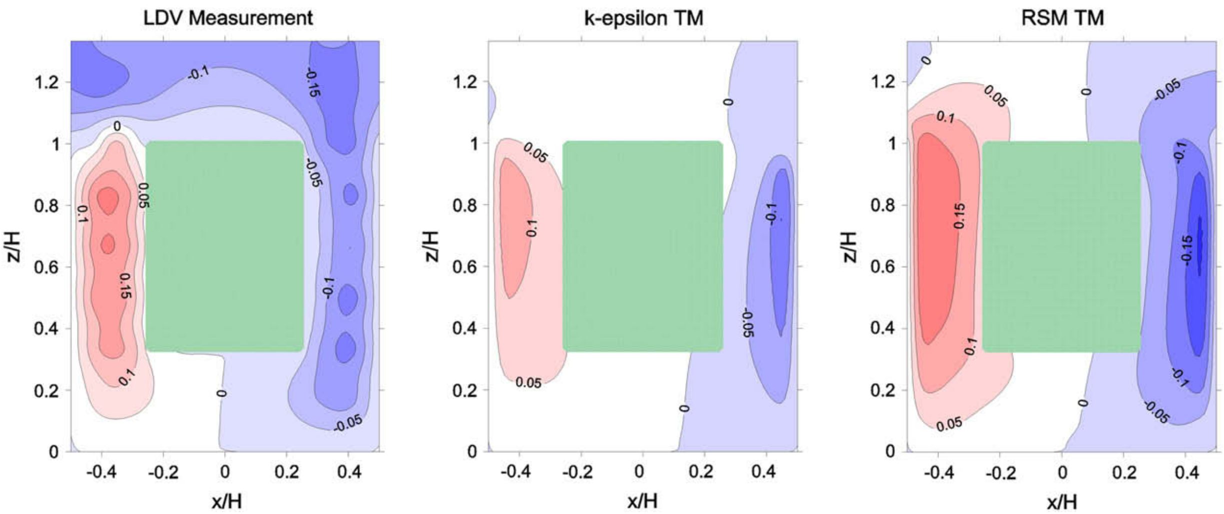

Fig. 8. Normalized vertical velocities w^+ at $y/H = 0.5$ in street canyon with porous tree crown model.

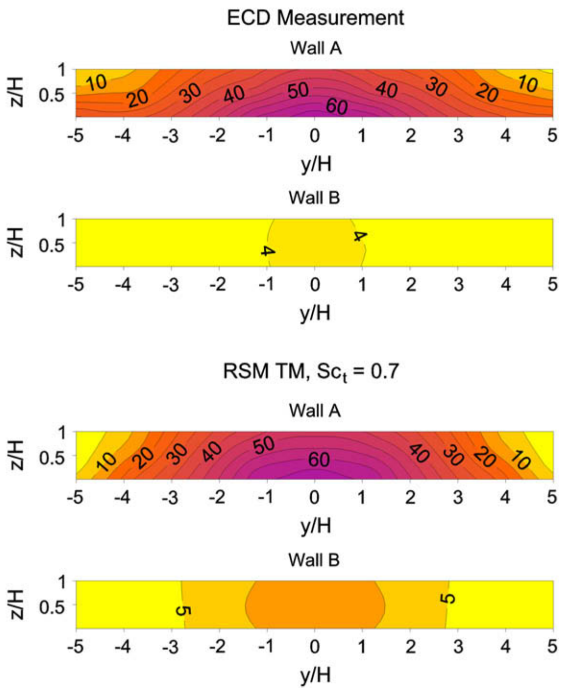

Fig. 9. Normalized concentrations c^+ at the walls of the street canyon with porous crown model.

3.3.2. Pollutant concentrations

The corresponding concentrations are shown in Fig. 9. Compared to the street canyon with non-porous tree crown arrangement (Fig. 7), both wind tunnel and numerical results showed no fundamental modifications. In fact, only slightly smaller maximum and wall-averaged pollutant concentrations at the leeward wall A are visible.

In conclusion, it can be stated that no essential deviations of the realized porous model porous crown from the solid model crown are present. Flow structures and pollutant transport mechanisms inside the street canyon do not differ significantly. Both models predict larger concentrations at wall B. However the RSM gives a better agreement with experiments than the k–ε model and for wall A, the best fit was achieved with the FLUENT default Sc_t value ($Sc_t = 0.7$).

3.4. Discussion and statistical analysis

The discrepancies between wind tunnel and numerical flow results are due to the poor prediction of the turbulence kinetic energy in the street canyon–roof top interface, which is lower than in the wind tunnel experiments. The vertical momentum exchange from the above roof flow downward to the street canyon is too small, resulting in too small shear force driving the canyon vortex which is consequently weaker than in the wind tunnel experiments. When less air is rotating with the canyon vortex, consequently larger pollutant concentrations have to be present in the street canyon when the pollutant source strength and the exchange rates at the canyon–roof interface are constant. Moreover, the steady state simulations did not predict the transient nature of the mixing process in the street canyons. This could be improved by performing non-stationary simulations, which are left to future investigations. However, in this work, our intention was to investigate the problem by using RANS models as we expect the applications of those models to air quality problems to increase in the next future and to replace nowadays integral and semi-empirical models.

The main results of the present study are summarized in Table 1 and Fig. 10. Table 1 gives the normalized volume fluxes at $z/H = 0.7$ near the canyon center at $y/H = 0.5$. Fig. 10 summarizes the wall-averaged pollutant concentrations resulting from the numerical computations and the wind tunnel measurements.

From Fig. 10a, it can be concluded that overall both the k–ε model and the RSM matches experimental data for a value of Sc_t equal to about 0.3 in the reference case of the tree-less street canyon. This is in satisfactory agreement with the value proposed by Di Sabatino et al. (2007), who found $Sc_t = 0.4$ appropriate for modeling pollutant dispersion in an urban street canyon when employing a k–ε model. In regard to the flow field, both turbulence models deliver lower flow velocities than those measured in the wind tunnel (Fig. 4), but no significant deviations between the k–ε model and the RSM can be found (Table 1).

In the street canyon configuration with non-porous model crown (Fig. 10b), pronounced differences in optimum turbulent Schmidt numbers are found. The best value of Sc_t is 0.6 when employing the RSM, while the k–ε model with this value did not produce satisfactory agreement with experimental results. The normalized volume fluxes presented in Table 1 clearly demonstrate the better performance of the RSM. This suggests a more complex structure of the dispersion process in the canyon which is not captured by the k–ε model.

The comparison of numerical and experimental results for the street canyon with porous model crown (Fig. 10c) confirms the better performance of the RSM model.

In order to asses the model performance, several statistical methods were used, such as the normalized mean square error (NMSE), the correlation coefficient (R), the fraction of predictions within a factor of two of observations (FAC2) and the fractional bias (FB), (Chang and Hanna, 2004). Recommendations for model acceptance criteria have been summarized and are given by: $\mathrm{NMSE} \leq 4$; $\mathrm{FAC2} \geq 0.5$; $-0.3 \leq \mathrm{FB} \leq 0.3$. For the suggested turbulent Schmidt numbers Sc_t, all statistical measures are within the accepted values for satisfactory model performance (Table 2).

In general, the results show that the k–ε model performs poorly when used to simulate flow and pollutant dispersion in street canyons with tree planting, while RSM

Table 1
Normalized volume fluxes (times 10,000) at $z/H = 0.7$ near the canyon center at $y/H = 0.5$

	Exp.	k–ε	RSM
Ref. case	693	482	474
Non-porous crown	250	122	204
Porous crown	267	192	311

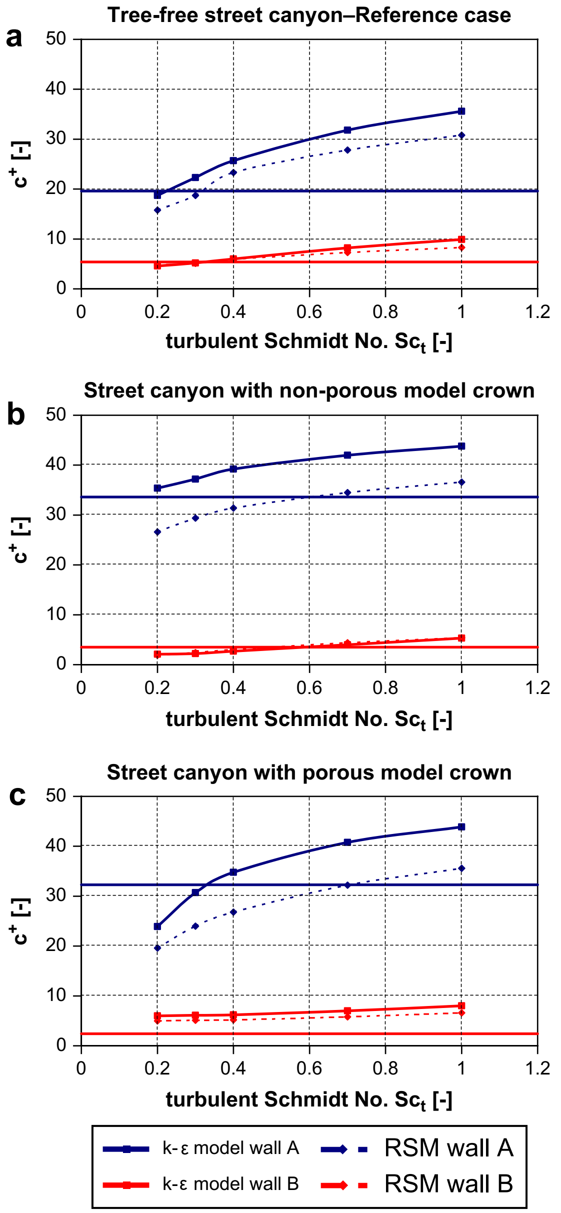

Fig. 10. Averaged-wall concentrations from FLUENT for different Sc_t (horizontal lines: wind tunnel results).

models might be adopted even though some extra investigations would be required. The general suggestions is that more complex turbulence models should be employed for this type of applications and most probably Large Eddy Simulations models would be more appropriate.

Results of this study are in general agreement with the numerical investigations of Gross (1997) and Ries and Eichhorn (2001). However, due to different underlying street canyon-tree planting configurations, a comparison is limited to more general characteristics. Gross (1997) investigated the influence of a tree planting consisting of two rows arranged sidewise of the street next to the building walls. Using a k–ε turbulence closure scheme and modeling the tree crowns by porous bodies, he found decelerated flow velocities near the building walls and increased pollutant concentrations inside the street canyon when compared to the setup without trees. In another numerical simulation of comparable tree arrangement, Ries and Eichhorn (2001) found local increases of the pollution concentration at the leeward wall accompanied by reduced flow velocities due to trees. They employed a special k–ε closure in which k was obtained from the well-known differential transport equation and ε from an algebraic relation involving the Blackadar mixing length formula. As before, by Gross (1997), tree crowns were modeled by porous bodies, but this time an additional term accounting for the enhanced production of turbulent kinetic energy inside the porous body was incorporated into the transport equation for the turbulent kinetic energy. However, in both investigations, 2-dimensional models were applied, which neither account for the 3-dimensional nature of turbulence nor for the highly 3-dimensional flow fields present in real urban street canyons of finite length. Furthermore, only individual cases and no variations in the tree planting configurations were considered. Experimental wind tunnel investigations of flow and concentration fields in urban street canyons of finite length with various avenue-like tree plantings were performed by Gromke and Ruck (2007, 2008). Systematical variations of crown diameter, height and porosity (permeability) were carried out. Measurements were performed by including as well as excluding traffic-induced turbulence. For perpendicular approaching flow, increases in pollutant concentrations at the leeward canyon wall and decreases in concentrations at the windward wall were found when compared to the tree-free street canyon. Air exchange and entrainment conditions were considerably modified, resulting in lower flow velocities and in overall larger pollutant charges inside the canyon. For crown porosities below a certain threshold, the tree planting impacts on the flow and concentration fields inside the canyon became independent of the degree of porosity and the tree planting behaved almost like an impermeable object.

Table 2
Results of statistical analysis with BOOT for the RSM

	NMSE	R	FAC2	FB
Tree-free ($Sc_t = 0.3$)	0.23	0.91	0.71	0.07
Non-porous crown ($Sc_t = 0.6$)	0.06	0.98	0.83	−0.004
Porous crown ($Sc_t = 0.7$)	0.09	0.97	0.53	−0.14

4. Conclusions

Flow fields and dispersion of traffic exhausts in urban street canyons with avenue-like tree planting were investigated by means of wind tunnel experiments and CFD investigations.

Results from wind tunnel measurements and numerical simulations showed reduced flow velocities and larger overall traffic exhaust concentrations were found in street canyons with avenue-like tree planting when compared to the tree-free counterpart. Large concentration increases at the inward canyon leeward wall and weak to moderate concentration decreases at the windward wall were measured. The performance of the RSM in predicting flow fields was better than the k–ε model, even if the computations generally predicted too low flow velocities and consequently the volume fluxes of circulating air masses inside the street canyons were underestimated. When employing the RSM model, a better agreement with wind tunnel concentration data was achieved by slightly lowering the turbulent Schmidt number in order to increase diffusion. Since most commercially available CFD codes operate with default values in the range of $Sc_t = 0.7$–1.0, the present study allows the recommendation that the turbulent Schmidt number should be critically reviewed when using standard turbulence models for pollutant dispersion investigations in urban areas.

Overall, this study suggests that the in-canyon air quality can be significantly altered by introducing tree planting in urban planning stage. In this context, the combination of experimental and numerical investigations can provide useful suggestions for assessment, planning and implementation of exposure mitigation in street canyons with tree planting.

Acknowledgements

The authors would like to express their thanks to the German Research Foundation DFG (Deutsche Forschungsgemeinschaft) for funding the part of this study, which was conducted at the University of Karlsruhe in Germany (Grant-no. Ru 345/28). The authors also thank Dr. Beatrice Pulvirenti for useful discussions. Thanks also go to two anonymous referees for reading the paper and for providing constructive and detailed comments and helping in improving the paper.

References

Ahmad, K., Khare, M., Chaudhry, K.K., 2005. Wind tunnel simulation studies on dispersion at urban street canyon and intersections – a review. Journal of Wind Engineering and Industrial Aerodynamics 95, 697–717.

Baik, J.J., Kim, J.J., 1999. A numerical study of flow and pollutant dispersion characteristics in urban street canyons. Journal of Applied Meteorology 38, 1576–1589.

Barth T.J., Jespersen D., 1989. The design and application of upwind schemes on unstructured meshes. Technical Report AIAA-89-0366. In: AIAA 27th Aerospace Sciences Meeting, Reno, Nevada.

Blocken, B., Stathopoulos, T., Carmeliet, J., 2007a. CFD simulation of the atmospheric boundary layer: wall function problems. Atmospheric Environment 41, 238–252.

Blocken, B., Carmeliet, J., Stathopoulos, T., 2007b. CFD evaluation of wind speed conditions in passages between parallel buildings-effect of wall-function roughness modifications for the atmospheric boundary layer flow. Journal of Wind Engineering and Industrial Aerodynamics 95, 941–962.

Chang, C., Meroney, R.N., 2003. Concentration and flow distributions in urban street canyons: wind tunnel and computational data. Journal of Wind Engineering and Industrial Aerodynamics 91, 1141–1154.

Chang, J., Hanna, S., 2004. Air quality model performance evaluation. Meteorology and Atmospheric Physics 87, 167–196.

Di Sabatino, S., Kastner-Klein, P., Berkowicz, R., Britter, R.E., Fedorovich, E., 2003. The modelling of turbulence from traffic in urban dispersion models – Part 1. Theoretical considerations. Environmental Fluid Mechanics 3, 129–143.

Di Sabatino, S., Buccolieri, R., Pulvirenti, B., Britter, R.E., 2007. Simulations of pollutant dispersion within idealised urban-type geometries with CFD and integral models. Atmospheric Environment 41, 8316–8329.

Di Sabatino, S., Buccolieri, R., Pulvirenti, B., Britter, R.E., 2008. Flow and pollutant dispersion modelling in street canyons using Fluent and ADMS-Urban. Environmental Modeling and Assessment 13, 369–381.

Eliasson, I., Offerle, B., Grimmond, C.S.B., Lindqvist, S., 2006. Wind fields and turbulence statistics in an urban street canyon. Atmospheric Environment 40, 1–16.

Fluent, 2005. V6.2 User's Manual. Available from: http://www.fluent.com.

Gao, Y., Chow, W.K., 2005. Numerical studies on airflow around a cube. Journal of Wind Engineering and Industrial Aerodynamics 93, 115–135.

Gerdes, F., Olivari, D., 1999. Analysis of pollutant dispersion in an urban street canyon. Journal of Wind Engineering and Industrial Aerodynamics 82, 105–124.

Gromke C., Ruck B., 2005. Die Simulation atmosphärischer Grenzschichten in Windkanälen. In: Proceedings of the 13th GALA Fachtagung Lasermethoden in der Strömungsmechanik, 51-1-51-8. German Association for Laser Anemometry.

Gromke, C., Ruck, B., 2007. Influence of trees on the dispersion of pollutants in an urban street canyon – experimental investigation of the flow and concentration field. Atmospheric Environment 41, 3287–3302.

Gromke, C., Ruck, B., 2008. On the impact of trees on dispersion processes of traffic emissions in street canyons. UAQ2007 Special Issue in Boundary Layer Meteorology, doi:10.1007/s10546-008-9301-2.

Gross, G., 1987. A numerical study of the airflow within and around a single tree. Boundary Layer Meteorology 40, 311–327.

Gross, G., 1997. ASMUS – Ein numerisches Modell zur Berechnung der Strömung und der Schadstoffverteilung im Bereich einzelner Gebäude. II: Schadstoffausbreitung und Anwendung. Meteorologische Zeitschrift 6, 130–136.

Hanna, S.R., Tehranian, S., Carissimo, B., Macdonald, R.W., Lohner, R., 2002. Comparisons of model simulations with observations of mean flow and turbulence within simple obstacle arrays. Atmospheric Environment 36, 5067–5079.

Kastner-Klein, P., Plate, E.J., 1999. Wind-tunnel study of concentration fields in street canyons. Atmospheric Environment 33, 3973–3979.

Kastner-Klein, P., Fedorovich, E., Rotach, M.W., 2001. A wind tunnel study of organised and turbulent air motions in urban street canyons. Journal of Wind Engineering and Industrial Aerodynamics 89, 849–861.

Launder, B.E., Spalding, D., 1974. The numerical computation of turbulent flows. Computer Methods in Applied Mechanics and Engineering 3, 269–289.

Launder, B.E., 1989. Second-moment closure: present and future? International Journal of Heat Fluid Flow 10 (4), 282–300.

Li, X., Liu, C., Leung, D.Y.C., Lam, K.M., 2006. Recent progress in CFD modelling of wind field and pollutant transport in street canyons. Atmospheric Environment 40, 5640–5658.

Meroney, R.N., Pavageau, M., Rafailidis, S., Schatzmann, M., 1996. Study of line source characteristics for 2-D physical modelling of pollutant dispersion in street canyons. Journal of Wind Engineering and Industrial Aerodynamics 62, 37–56.

Pavageau, M., Schatzmann, M., 1999. Wind tunnel measurements of concentration fluctuations in an urban street canyon. Atmospheric Environment 33, 3961–3971.

Ries, K., Eichhorn, J., 2001. Simulation of effects of vegetation on the dispersion of pollutants in street canyons. Meteorologische Zeitschrift 10, 229–233.

Ruck, B., Schmidt, F., 1986. Das Strömungsfeld der Einzelbaumumströmung. Forstwissen-schaftliches Centralblatt 105, 178–196.

So, E.S.P., Chan, A.T.Y., Wong, A.Y.T., 2005. Large-eddy simulations of wind flow and pollutant dispersion in a street canyon. Atmospheric Environment 39, 3573–3582.

Tominaga, Y., Stathopoulos, T., 2007. Turbulent Schmidt numbers for CFD analysis with various types of flowfield. Atmospheric Environment 41, 8091–8099.

Vardoulakis, S., Fisher, B.E.A., Pericleous, K., Gonzalez-Flesca, N., 2003. Modelling air quality in street canyons: a review. Atmospheric Environment 37, 155–182.

Zhou, X.H., Brandle, J.R., Takle, E.S., Mize, C.W., 2002. Estimation of the three-dimensional aerodynamic structure of a green ash shelterbelt. Agricultural and Forest Meteorology 111, 93–108.